

# Physical Performance of Cement-Treated Silty Sand Soil under Cycles of Freezing/Thawing

Reza Jolous Jamshidi, Craig B. Lake, Chris Barnes,  
*Civil and Resource Engineering Department, Dalhousie University,  
Canada*

Colin D. Hills, Peter Gunning  
*Centre for Contaminated Land Remediation, University of Greenwich,  
United Kingdom*



## ABSTRACT

Cement-based solidification/stabilization (S/S) is becoming an increasingly used technology for treatment of a wide range of contaminants. Current design of S/S remediation systems to resist freeze/thaw (f/t) cycles is based on tests available for soil-cement which considers sample's integrity (rather than its hydraulic properties) as the resistibility indicator. This paper studies the effect of f/t cycles on physical performance of a silty sand soil solidified by addition of 10 percent Portland cement. Changes in the hydraulic conductivity, dynamic properties and micro-structure of the specimens were monitored after exposure to different levels of f/t. Results show a considerable amount of damage to the structure of the monolith after 7 cycles of f/t. An increase of up to two orders of magnitude in the hydraulic conductivity of the specimens was observed. Also changes in the dynamic properties of the specimens suggest the proposed technique may be suitable for detection of performance change due to f/t exposure.

## RÉSUMÉ

La solidification/stabilisation ciment-basé (le S/S) devient une technologie de plus en plus utilisée pour le traitement d'une grande variété de contaminants. La conception actuelle de systèmes de redressement de S/S pour résister le gèle/dégel (f/t) les cycles sont fondés sur les tests disponibles pour le sol-ciment qui considère l'intégrité de l'échantillon (au lieu de ses propriétés hydrauliques) comme l'indicateur de resistibility. Ce papier étudie l'effet de cycles de f/t sur l'exécution physique d'un sol de sable de silty solidifié par l'addition de ciment de Portland de 10 pourcent. Les changements dans la conductivité hydraulique, les propriétés et la micro-structure dynamiques des spécimens ont été contrôlées après l'exposition aux niveaux différents de f/t. Les résultats montrent beaucoup de dommages à la structure du monolithe après 7 cycles de f/t. Une augmentation de jusqu'à deux ordres de magnitude dans la conductivité hydraulique des spécimens ont été observés. Aussi les changements dans les propriétés dynamiques des spécimens suggèrent que la technique proposée peut être convenable pour la détection de changement d'exécution en raison de l'exposition de f/t.

## 1. INTRODUCTION

Cement based solidification/stabilization (S/S) is a well-established remediation technology for the treatment of a wide range of contaminated soils/sludge (Paria and Yuet, 2006). The general technique of this technology involves mixing waste/contaminated soil with a binder (cement or other supplementary materials such as fly ash, furnace slag, etc.) to immobilize the contaminants in the structure of the resulting monolith (Bone et al., 2004). Immobilization of contaminants can occur as a result of changes in physical properties of the waste material (i.e. solidification) and/or chemical changes in the contaminant/matrix (i.e. stabilization) (Batchelor, 2006). Because of the potential advantages of this technology (i.e. economics, soil improvement, risk reduction, etc.), considerable research has been performed to investigate the effectiveness of the technology for treatment of different types of contaminants (e.g.: Chan et al., 2000; Silva et al., 2007, Leonard and Stegmann, 2010). However, little research has been published related to evaluation of the long term performance of this technology in cold regions where it is prone to exposure to cycles of freezing and thawing (f/t).

Freeze/thaw can occur either during the construction phase of the project (i.e. prior to cover system placement), or at some point during the design life; when the cover system fails to fulfill its purpose as an insulation barrier. Both of these scenarios are a concern for Canada, as cement-based S/S projects have received increased attention in recent years for the remediation of Brownfield sites (e.g. The Sydney Tar Ponds remediation project, Sydney, Nova Scotia).

Despite the lack of experience on the performance of cement-based S/S monolith materials subjected to f/t, there is considerable research related to the f/t effects on compacted clays for landfill applications (e.g.: Othman and Benson, 1992; Othman and Benson, 1993), soil-cement for transportation applications (e.g.: Yarbasi et al., 2007; Shihata and Baghdadi, 2001; Kettle, 1986) and concrete (e.g.: Penttala 2006; Micahhale et al., 2009). Generally, the understanding of a cement-based material exposed to sub-zero temperatures is that initially the water in large pores (entrapped/entrained pores) and subsequently capillary pores will freeze (Chatterji, 2003). Freezing of water results in an increase in the initial volume and this can create internal forces within the structure (Chatterji, 2003) which potentially can cause damage of the cement-based material.

Previous work investigating the influence of f/t on the durability of cement-based S/S materials include that by Klich et al. (1999) who used microscopic techniques to show how weathering processes such as f/t can cause cracking of these materials. Stegman and Cote (1996) proposed a protocol for the assessment of S/S wastes under f/t exposure conditions. In this proposed method, specimens which survive 12 f/t cycles with less than 10 percent mass loss due to manual brushing at the end of each cycle are considered to pass the required criteria for f/t resistibility. This test, however, does not provide any information on the changes in the hydraulic performance of exposed specimens. There are also few studies that have examined the mechanisms responsible for decreased hydraulic performance for cement-based S/S monolith materials under f/t exposure conditions.

The objectives of this paper are threefold: firstly to evaluate the development of changes in the laboratory hydraulic performance of cement-based S/S monoliths due to cycles of f/t; secondly, to use microscopic techniques to provide some explanation of the mechanisms involved in the damage development observed; and thirdly, to show the ability of a non-destructive test to assess this damage development in these materials during f/t exposure.

## 2. MATERIALS AND METHODS

### 2.1 Soil characterization and specimen preparation

Silty sand soil (ASTM D2487) from Windsor, Nova Scotia was used in this study. Minor amounts of clay were present in the soil but insufficient amounts were present to contribute to the soil classification. Portland cement Type 10 (GU) was used in the cement treatment process. A water/cement ratio of 2.28 and cement content of 10 percent (dry weight cement/dry weight of soil) was used in the mix design. Cement and water were proportioned and mixed together for 1 minute using a drill mixer in a bucket, to ensure the uniform distribution of cement within the final product. The soil was then added in small portions and mixed until visually homogeneous. The soil-cement mixture was then placed into 101 mm diameter by 118 mm length plastic molds which were previously lubricated with a thin film of oil to ease the de-molding process. The mixture was placed in three approximately equal layers, each subjected to 20 rod strokes to provide consistent consolidation for each layer. After the placement of final layer, the surface of the specimens were smoothed, plastic caps were placed on the molds, and samples were placed in sealed plastic bags for 5 days prior to extrusion from the molds. The specimens were extruded from molds using pressurized air and placed in a concrete moist-curing room for 110 days. This was done to ensure that hydration was essentially complete prior to the start of f/t conditioning and hydraulic conductivity testing.

### 2.2 Freeze/thaw conditioning

Confirmation that complete freezing and thawing was occurring during f/t conditioning of samples cycle was

achieved by monitoring the internal temperature of a sacrificial specimen. Results showed complete freezing and thawing occurred within the total cycle length of 48 hours chosen for this study. F/t conditioning included 24 hours of freezing the specimens in a cold room at a temperature of  $-10 \pm 1$  °C followed by thawing in a 100% humidity room at room temperature ( $22 \pm 1$  °C). During the thawing stage, the specimens were allowed to absorb ambient moisture from the humidity room.

Initial plan was to continue the f/t conditioning to 12 cycles. A total of eight specimens were prepared for this purpose. Four of these specimens (i.e. repeat tests) were used for monitoring the changes in hydraulic conductivity and dynamic characteristics at 0, 1, 2, and 4 f/t cycles (i.e. hydraulic conductivity followed by impact resonance test at cycles of interest). The remaining four specimens were used for microscopic evaluation of changes due to exposure at the different f/t levels. However, due to extensive damage of the specimens after 7 f/t cycles, additional testing was not possible.

### 2.3 Hydraulic conductivity testing

The hydraulic conductivity of the specimens were measured according to ASTM D5084 (Flexible-wall method), using saturation, consolidation and permeation stages. Back-pressure saturation was performed under an effective confining pressure of 35 kPa, followed by consolidation under effective confining pressures of 138 kPa. Subsequent permeation with distilled water was performed under a gradient of 35 kPa. Termination criteria according to ASTM 5084 were used to determine final hydraulic conductivity test values.

### 2.4 Microscopy

The extent of f/t damage to the waste form microstructure was investigated using a combination of scanning electron microscopy (SEM) and petrographic examination using optical microscopy.

Replicate thin sections were prepared from resin impregnated specimens taken from the control sample, and samples subjected to 1 and 4 f/t cycles.

Samples were examined using a Nikon Optiphot-Pol polarized light microscope. Images were collected using a 12 megapixel digital scanning camera (Kontron ProgRes 3012) with the ProgRes acquisition software.

A second set of thin sections (without cover slips) were carbon coated for SEM analysis (Edwards Carbon Coater). SEM analysis was performed on a JEOL JSM-5310LV microscope equipped with an Oxford Instruments Energy Dispersive Spectrometer (EDS). The accelerating voltage was 20kV, with a working distance of 15mm. Backscattered electron images and energy dispersive analysis of x-rays were acquired using Oxford ISIS image acquisition and analytical software.

### 2.5 Impact resonance testing

To investigate the development of damage during the exposure process, impact resonance testing was

performed. This is a non-destructive test which has been widely used to predict changes in the performance and dynamic properties (including natural frequency and damping ratio) of different materials (e.g.: Nieto et al. 2006; Whitmoyer and Kim, 1994). ASTM C666 suggests a similar technique to measure changes in the dynamic modulus of elasticity of concrete beams after exposure to rapid cycles of  $f/t$ .

Figure 1 shows the set-up used for the impact resonance test in the current study. During the test, the specimens were supported on a rectangular sponge measuring 23X9X7 cm. A 1X1 cm square piece of steel, thickness of 1 mm, was glued to the centerline of the specimen on both sides to enable the magnetic connection of an accelerometer to the sample for measuring the longitudinal vibration of the cylindrical specimen. The steel square also provided a hard base upon which to create an elastic impact on the samples. The specimen was excited using a steel ball with a diameter of 9.5 mm glued to a plastic band (a combined mass of approximately 5.3 gram). The response signal was acquired using an accelerometer (PCB model 353B02) connected to the other side of the specimen which transferred the signals to an amplifier and a computer (Freedom Data PC Platform, Olson Instruments Inc.) for signal processing. A sampling rate of 2 micro seconds, record size of 8192 samples and bandwidth filter with a minimum frequency of 500 and maximum frequency of 10000 was applied during the test. During each test, signals were processed in the computer's software using a Fast Fourier Transform (FFT) to calculate the damped frequency of each specimen. Each test consists of five trials on the specimen. Testing was performed on the four specimens after each hydraulic conductivity test after the 0, 1, 2, and 4<sup>th</sup>  $f/t$  cycle.

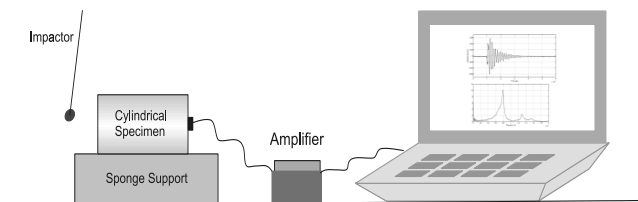


Figure 1- Impact-resonance test configuration

The normalized changes in the longitudinal damped frequency at the  $m^{\text{th}}$  cycle of  $f/t$  ( $\Delta_{f_D}^m$ ), are reported in this paper based on the following equation:

$$\Delta_{f_D}^m = \frac{f_D^m}{f_D^o} \quad [1]$$

Where  $f_D^m$  and  $f_D^o$  are damped frequencies at the  $m^{\text{th}}$  cycle of  $f/t$  and control specimens respectively.

Raw data from the impact resonance test were extracted from the software and further processed to calculate the damping ratio of the specimens. The damping ratio can be calculated using the logarithmic decrement method (Buchholdt, 1997). In this method the logarithmic decrement in the acceleration-time domain of the response signal can be calculated using equation 2.

$$\delta = \frac{1}{j} \times \ln\left(\frac{A_i}{A_{i+j}}\right) \quad [2]$$

In which  $A_i$  and  $A_{i+j}$  are the peak amplitudes at  $i^{\text{th}}$  and  $(i+j)^{\text{th}}$  number of cycles in the acceleration-time domain.

This value can be used in equation 3 to calculate the damping ratio,  $\xi$ .

$$\xi = \frac{1}{\sqrt{1 + \left(\frac{2\pi}{\delta}\right)^2}} \quad [3]$$

A Matlab code was created to locate the peaks (both local maximums and minimums) in the acceleration waveform. The absolute value of these peaks at a distance of half a cycle in the acceleration-time domain (i.e.  $j=0.5$ ) were then incorporated into Equation 2 to calculate the value of  $\delta$ . This was specifically required for the damaged specimens as the number of available peaks in the acceleration-time domain was significantly reduced because of the high damping capacity. The values of damping ratio were then calculated using equation 3. These values were then averaged for each specimen.

Damping ratios can be applied to the damped frequency values to calculate the natural frequency,  $f_n$ , of the system:

$$f_n = f_D \sqrt{1 + \xi^2} \quad [4]$$

Where:  $f_D$  is damped frequency of the system.

However for most cases of under-damped systems, the values of natural and damped frequency are within a close range (compared to the changes resulting from the damage). As a result, the current paper results of the damped frequencies at different  $f/t$  exposure levels are compared.

### 3. RESULTS

Changes in both performance and the structure of stabilized samples were observed in the tests. As was previously discussed, it was planned to continue the tests for 12 cycles of  $f/t$  exposure. However after 4  $f/t$  cycles,

the amount of specimen degradation was to an extent that further handling of the specimens for different tests was not possible. Hence, the current paper only presents the results of observations up to 4 f/t cycles. Figure 2 presents a photo of a specimen, typical of the amount of physical damage after 7 cycles of f/t exposure.



Figure 2- Degradation of a specimen after 7 f/t cycles

### 3.1 Hydraulic conductivity

One of the main objectives of cement-based S/S treatment of contaminated soils is to decrease the hydraulic conductivity of the mixture such that the contaminant release would mainly be controlled by the diffusion process. USEPA (1997) suggests a maximum hydraulic conductivity value of  $10^{-8}$  m/s in the design of S/S products. In this study, the cement treated soils had an initial hydraulic conductivity value of  $1.2 \times 10^{-10}$  m/s (average of the 4 samples). As shown in Figure 3, after one f/t cycle, the largest increase in hydraulic conductivity value was observed. Increases in hydraulic conductivity, albeit at a slower rate, were also observed for subsequent f/t cycles, as shown on Figure 3. Values approached  $10^{-8}$  m/s at the end of 4 cycles; approximately 100 times larger than the initial hydraulic conductivity of the samples.

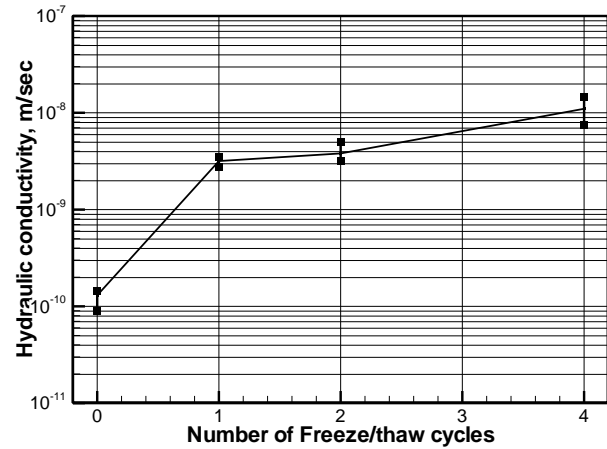


Figure 3- Hydraulic conductivity results of samples after exposure to 0, 1, 2, and 4 f/t cycles

### 3.2 Electron and optical microscopy

An examination of the microstructure of the cement-treated soil by optical microscopic techniques enabled insight into how the waste form matrix was disrupted on exposure to f/t cycling. The control sample (0 cycles) shown in Figures 4 (transmitted light micrograph) and Figure 5 (backscattered electron micrograph) exhibited soil particles encapsulated in a dense matrix of hydration products. These particles included angular to sub-rounded quartz grains, weathered igneous and metamorphic rocks and shocked quartz; many were iron stained. Several (>mm) grains composed of feldspar were noted.

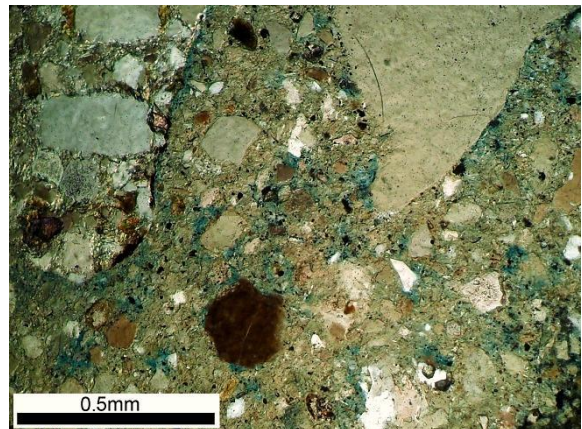


Figure 4 – Transmitted light micrograph of the control sample (note the blue color results from the resin used for impregnation of the sample prior to polishing)

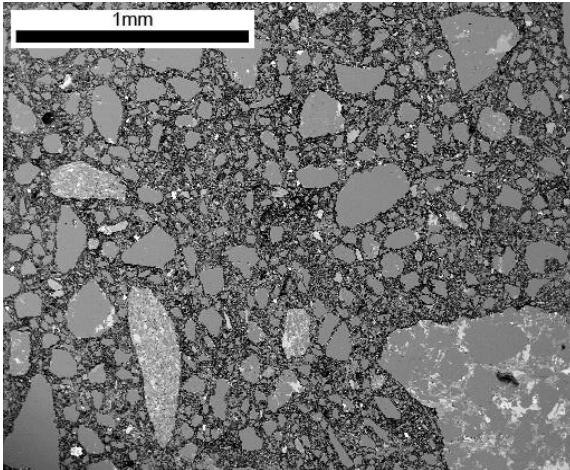


Figure 5 – Backscattered electron micrograph of the sample

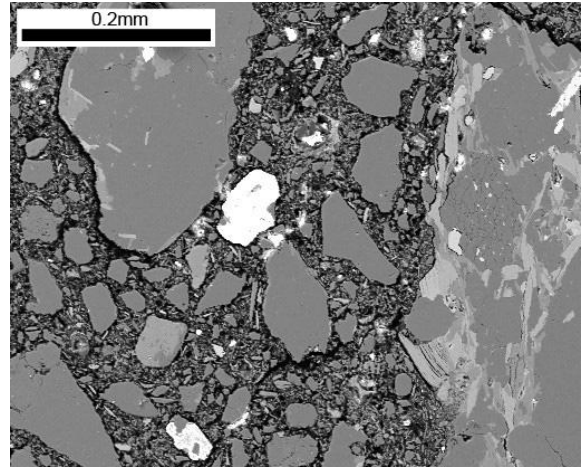


Figure 7 – Backscattered electron micrograph of the sample exposed to 1 cycle

Figures 6 and 7 show transmitted light and backscattered electron micrographs of the cement-solidified soil exposed to 1 f/t cycle, respectively. The most notable feature was the appearance of extended cracks primarily located found in the sample matrix close to, or following grain boundaries. Occasionally, cracks cut across individual (larger) soil particles. These cracks had a frequency of approximately 1.2mm, and a crack width of 0.03-0.05mm.

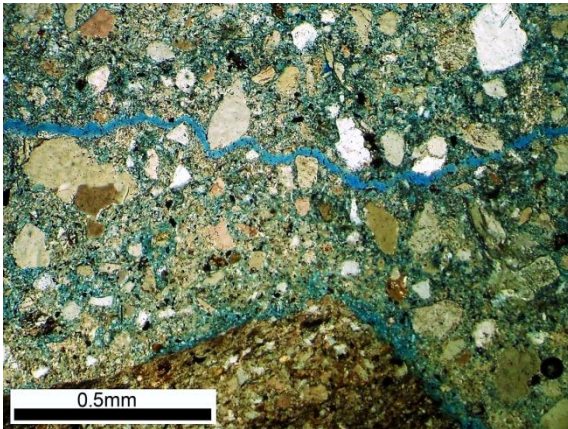


Figure 6 – Transmitted light micrograph of the sample exposed to 1 cycle. (Note: a crack, located within the sample matrix, is clearly seen transverse the field of view from W to E).

The enhanced disruption resulting from 4 cycles of f/t was very noticeable, especially under transmitted light (Figure 8). The blue resin used enabled the developing crack network to be easily observed. Degradation of the matrix at greater distances ( $\geq 0.5\text{mm}$ ) from the primary crack(s) was evident. Figure 9 shows the 4 f/t cycle sample, with a crack “snaking” NW-SE across the sample. The matrix appears darker (i.e. is less dense) in this backscattered electron micrograph, confirming that the zone of disruption is extending outwards into previously unaffected parts of the matrix. This form of disruption is progressive and will result in complete degradation of the sample matrix in the extreme case.

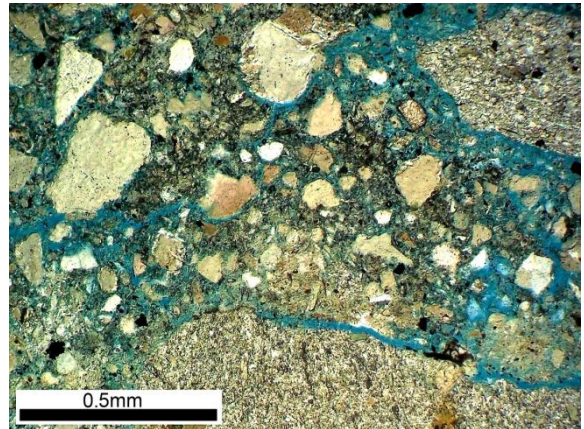


Figure 8 – Transmitted light micrograph of the sample exposed to 4 cycles (Note: significant disruption of the matrix by cracking – dark areas show resin impregnated voids)

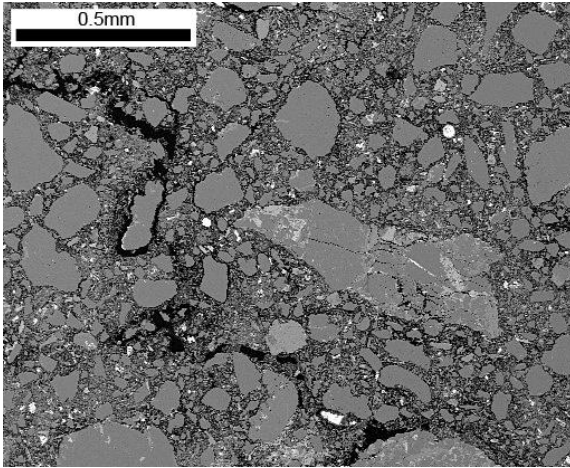


Figure 9 – Backscattered electron micrograph of the sample exposed to 4 cycles (note: darker areas are porous and extend inwards along the crack boundary, showing enhanced matrix disruption)

### 3.3 Impact-resonance results

The previous sections have identified increases in hydraulic conductivity with f/t cycles and have shown how micro-cracks are likely a contributing factor for this increase. To be able to detect potential damage of hydraulic performance due to f/t cycles, impact resonance represents a relatively simple test to perform to assess this damage. Shifts in the natural frequency of a cement-based S/S monolith material can represent changes in the monolith which can be a result of damage (reduction in the frequency) or curing (increase in the frequency). This is due to the natural frequency being proportional to the modulus of elasticity of the material. As well, the damping ratio represents the energy dissipation characteristics of the system. In an undamaged system, the energy created by the impact is mainly utilized for the vibratory motion of the system. In a damaged system due to the presence of defects, dissipation of the energy occurs in a shorter time period (Razak and Choi, 2001).

Figure 10-a presents a typical response spectrum for an undamaged specimen used in this study. The frequency distribution of this response is presented in Figure 10-b.

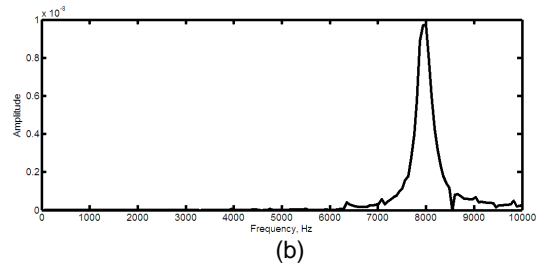
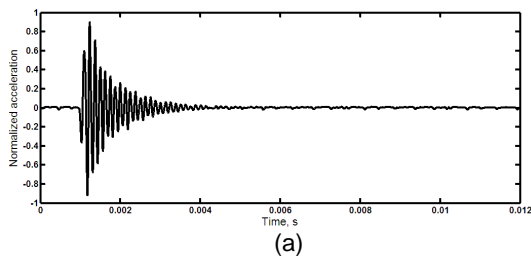


Figure 10 – Dynamic test on an undamaged specimen  
a) Acceleration time domain b) Frequency response

The average changes in the normalized damped frequency of specimens at different f/t exposures are presented in Figure 11. Similar to hydraulic conductivity, the damped frequency of the specimens showed a considerable change after the first f/t cycle and it continued to decrease (with slower rate) at the later exposures. An interesting observation is that the shape of Figure 11 looks similar to that of Figure 5 in terms of rate of increase of hydraulic conductivity.

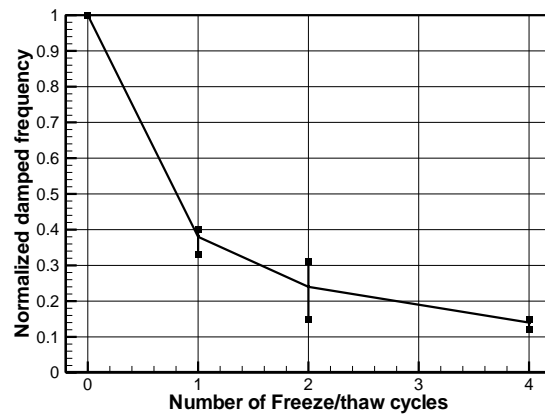


Figure 11 – Changes in the normalized damped frequency at different f/t cycles

The damping ratio was calculated by analyzing the time domain acceleration waveform. Average values and observed ranges for the damping ratio of the specimens at different f/t cycles are presented in Table 1.

Table 1. Average values for the damping ratio at different levels of f/t exposure

Number of freeze/thaw cycle	Damping ratio ( $\xi$ )	Damping ratio range
0	0.06	0.05-0.07
1	0.18	0.12-0.24
2	0.27	0.23-0.30
4	0.41	0.33-0.48

It was observed that exposure to f/t cycles can highly increase the damping capacity of the specimens which

may be the result of development of voids/cracks in the matrix. However there is a high variability between different specimens which may be a result of sensitivity of this value on the damage distribution/direction in the structure. More work is required to develop this technique.

#### 4. CONCLUSION

In this study, physical performance of a cement-treated silty-sand soil was evaluated under exposure to up to four cycles of freezing at  $-10\pm 1^{\circ}\text{C}$  and thawing at room temperature. The following observations were made from these results:

- Results showed an increase of up to two orders of magnitude in the hydraulic conductivity of the specimens after exposure to 4 cycles of f/t. Also, values of damped frequency and damping ratio showed a decrease of 88 percent and an increase of approximately seven-fold respectively.
- Samples showed disruption from as little as 1 cycle of f/t through the introduction of an extended longitudinal crack network, with a spacing of approximately 1.2mm. After 4 f/t cycles it was observed that further disruption of the matrix had occurred and the matrix had become degraded some distance from crack boundaries.
- Both hydraulic conductivity and dynamic test results showed that a considerable amount of the damage can be expected after the first f/t cycle. However, the damaging process continues at further exposures, albeit at a smaller rate.
- Both damped frequency and damping ratio seem to be reliable tools for monitoring the development of physical damage in S/S materials due to exposure to cycles of f/t. However, appropriate correlations between the results and hydraulic conductivity values need to be established. Use of the proposed technique can eliminate the uncertainty involved in the current practices for evaluation of S/S materials under f/t, which involves the manual brushing of the specimens.

The results presented in this study were for a given soil type and cement content. Further research is necessary to assess the influence of different scenarios of f/t exposure, soil type and mix design on the physical and chemical performance of cement S/S soils.

#### REFERENCES

- ASTM C666, 1997. Standard test method for resistance of concrete to rapid freezing and thawing. *Annual book of ASTM standards*, ASTM International. West Conshohocken, PA.
- ASTM D2487, 2010. Standard Practice for Classification of Soils for Engineering Purposes (Unified Soil Classification System). *Annual book of ASTM standards*, ASTM International. West Conshohocken, PA.
- ASTM D5084, 2000. Standard test methods for measurement of hydraulic conductivity of saturated porous materials using a flexible wall permeameter. *Annual Book of ASTM Standards*. ASTM International, West Conshohocken, PA.
- Batchelor, B. 2006. Overview of waste stabilization with cement. *Waste management*. 26 (7): 689-98.
- Bone, B.D., Barnard L.H., Boardman D.I., Carey, P.J., Hills, C.D., Jones, H.M., MacLeon, C.L., Tyrer, M., 2004. *Review of Scientific Literature on the Use of Stabilisation/Solidification for the Treatment of Contaminated Soil, Solid Waste and Sludges*. British Environmental Agency. SC980003/SR2.
- Buchholdt H.A. 1997. *Structural Dynamics for Engineers..* Thomas Telford, London, UK.
- Chan, Y.M., Agamuthu, P., Mahalingam, R. 2000., Solidification and stabilization of asbestos waste from an automobile brake manufacturing facility using cement, *Journal of Hazardous Materials*, 77(2): 209-226.
- Chatterji, S. 2003. Freezing of Air-Entrained Cement-Based Materials and Specific Actions of Air-Entraining Agents. *Cement and Concrete Composites*, 25(7):759-765.
- Kettle, R.J., 1986, Assessment of Freeze-thaw Damage in Cement Stabilized Soils. Conference Proceeding: *Research on Transportation Facilities in Cold Regions*. Boston, Massachusetts, 16- 31.
- Klich, I., Wilding, L.P., Drees, L.R., Landa, E.R. 1999. Importance of Microscopy in Durability of Solidified and Stabilized Contaminated Soils. *Soil Science Society American Journal*, 63:1274-1283.
- Leonard, S.A. and Stegemann, J.A. 2010. Stabilization/solidification of petroleum drill cuttings, *Journal of Hazardous Materials*. 174(1-3): 463-472.
- Micahhale, W, Freyne S., Russell B. 2009. Examining the frost resistance of high performance concrete. *Construction and Building Materials*. 23(2): 878-888.
- Nieto, a.J, Chicharro, J.M, Pintado, P. 2006. An approximated methodology for fatigue tests and fatigue monitoring of concrete specimens. *International Journal of Fatigue*. 28(8):835-842.
- Othman, M.A. and Benson C.H. 1992. Effect of Freeze-Thaw on the Hydraulic Conductivity of Three Compacted Clay from Wisconsin. *Transportation Research Board. Advances in Geotechnical Engineering*, 1369: 126-129.
- Othman M.A. and Benson C.H., 1993, Effect of Freeze-Thaw on the Hydraulic Conductivity and Morphology of Compacted Clay. *Canadian Geotechnical Journal*, 30:236-246.
- Paria, S. and Yuet, P.K., 2006. Solidification / Stabilization of Organic and Inorganic Contaminants using Portland cement: A Literature Review. *Environmental reviews*. 14: 217-255.
- Penttala, V. 2006. Surface and internal deterioration of concrete due to saline and non-saline freeze-thaw loads, *Cement and Concrete Research*. 36: 921-928.
- Razak, H.A. and Choi, F.C. 2001. The effect of corrosion on the natural frequency and modal damping of reinforced concrete beams, *Engineering Structures*, 23(9):1126-1133.

- Shihata, S.A. and Baghdadi, Z.A. 2001. Simplified Method to Assess Freeze-Thaw Durability of Soil Cement. *Journal of Materials in Civil Engineering*. 13(4):243-247.
- Silva M.A.R., Mater L., Souza-Sierra M.M., Correa A.X.R., Sperb R., Radetski C.M. 2007. Small hazardous waste generators in developing countries: use of stabilization/solidification process as an economic tool for metal wastewater treatment and appropriate sludge disposal, *Journal of Hazardous Materials*, 147(3):986-990.
- Stegemann, A. and Cote, P.L. 1996. A proposed protocol for evaluation of solidified wastes. *The Science of the Total Environment*. 178:103-110.
- USEPA, 1997. *Innovative site remediation technology-Stabilization/Solidification, Design and application*, Vol. 4, EPA 542-B-97-007.
- Whitmoyer, S.L. and Kim, Y.R. 1994. Determining asphalt concrete properties via impact resonance method. *Journal of Testing and Evaluation, ASTM International*. 22(2):139-148.
- Yarbasi, N., Kalkan, E., Akbulut, S. 2007. Modification of the Geotechnical Properties, as Influenced by Freeze-Thaw, of Granular Soils with Waste Additives. *Cold Regions Science and Technology*. 48(1):44-54.